NRC Research Press

ARTICLE

The addition of terminal alkynes to dimesitylfluorenylidenegermane

Nada Y. Tashkandi, Laura C. Pavelka, Margaret A. Hanson, and Kim M. Baines

Abstract: A variety of terminal alkynes were added to dimesitylfluorenylidenegermane, $Mes_2Ge{=}CR_2$ (where CR_2 = fluorenylidene). The addition of phenylacetylene and 1-hexyne to $Mes_2Ge{=}CR_2$ gave a germacyclohexene via a cycloaddition where the germene acts as the 4π component and the alkyne as the 2π component. Through the use of a mechanistic probe, *trans*-(2-phenylcyclopropyl)-acetylene, the reaction was postulated to proceed through a concerted [2+4] cycloaddition. The addition of ethoxyacetylene to the germene produced both a [2+2] cycloadduct, a germacyclobutene, and a [2+4] cycloadduct, a germacyclohexene. The results of this study are compared to the results of the addition of alkynes to $Mes_2Ge{=}CHCH_2$-*t*-Bu.

Key words: germene, alkyne, cycloaddition, mechanism.

Résumé : Divers alcynes terminaux ont été ajoutés au dimesitylfluorenylidènegermane, $Mes_2Ge{=}CR_2$ (où CR_2 = fluorenylidène). L'addition du phénylacetylène et du hex-1-yne au $Mes_2Ge{=}CR_2$ a produit un germacyclohexène par une cycloaddition lors de laquelle le germène agit comme le composant 4π et l'alcyne comme le composant 2π. En utilisant une sonde mécanistique, *trans*-(2-phénylcyclopropyl)acétylène, on suppose que la réaction s'effectue par l'intermédiaire d'une cycloaddition concertée [2+4]. L'addition d'éthoxyacetylène au germène a produit à la fois un cycloadduit [2+2], le germacyclobutène, et un cycloadduit [2+4], le germacyclohexène. Les résultats de la présente étude sont comparés à ceux de l'addition d'alcynes au $Mes_2Ge{=}CHCH_2$*t*-Bu. [Traduit par la Rédaction]

Mots-clés : germène, alcyne, cycloaddition, mécanisme.

Introduction

Cycloaddition reactions of group 14 metallenes have been attracting the interest of chemists for more than 40 years due to the high levels of regio- and stereospecificity.[1] The addition of alkynes to Brook silenes $(Me_3Si)_2Si{=}C(R)(OSiMe_3)$ is a classic example; the reaction produces silacyclobutenes rapidly and quantitatively (Scheme 1).[2] Through the use of a phenyl cyclopropyl-substituted alkyne mechanistic probe,[3] the cycloaddition of alkynes to Brook silenes was determined to proceed via a biradical intermediate.[4]

In contrast, when a variety of terminal alkynes were added to the neopentylsilene **1**, a preference for the formation of a C–H insertion product over the formation of formal ene and/or [2+2] cycloadduct(s) was observed (Scheme 2).[5]

A comparison between the reactivity of neopentylsilene **1** with that of neopentylgermene **2** towards alkynes revealed similar activity. Like silene **1**, three different modes of reactivity were observed for germene **2**: insertion of the acetylenic C–H bond to give germylacetylenes **3**, ene addition to give vinylgermanes **4**, and cycloaddition to give germacyclobutenes **5** (Scheme 3).[6]

A biradical pathway was proposed to account for the formation of the cycloadducts with aromatic alkynes based on the effect of the substituents on the rate of the reaction.[6] A chain reaction mechanism was proposed to explain the rapid formation of germylacetylenes (**3**). The initiator of the reaction is believed to be a trace amount of a strong base, creating the acetylide anion, which then adds to germene **2** producing the α-germyl carbanion **6**. The carbanion can deprotonate another equivalent of alkyne, reforming an acetylide anion, and the cycle can continue until it is quenched, presumably by residual $Mes_2GeF(CH{=}CH_2)$ (**7**; Scheme 4).[6]

The presence of the α-hydrogen in germene **2** facilitates the formation of the ene adduct **4**, while the basicity of the anion generated from **2** (**6**) leads to the CH-insertion product **3**. In contrast, dimesitylfluorenylidenegermane, **8**, lacks an α-hydrogen, which should eliminate the formation of ene-type adducts. Moreover, the amount of C–H insertion product may be reduced since the corresponding anion is less basic than anion **6**. Thus, we examined the addition of terminal alkynes to dimesitylfluorenylidenegermane, **8**, with the expectation that the reactions will not be as complex as those of germene **2**.

Mechanistic studies of metallenes are challenging: the reactivity of metallenes towards air and moisture as well as many common functional groups limits the variability of substituents and solvents that can be utilized. Our group has employed cyclopropyl-based hypersensitive mechanistic probes as a means to understand the reactivity of metallenes and their reaction pathways. *Trans*-(2-phenylcyclopropyl)acetylene[3] can be used as a probe to detect the formation of a reactive vinylic intermediate. During the cycloaddition of the alkyne moiety, rapid and regioselective cyclopropyl ring opening can occur upon the formation of a vinylic biradical or cationic intermediate. In contrast, no rearrangement of the probe will occur during a concerted addition. Thus, the isolation of ring-opened adducts of the alkyne probe provides strong evidence for the formation of an intermediate. In an attempt to elucidate the mechanism of the addition of alkynes to germenes, we

Received 15 November 2013. Accepted 19 February 2014.

N.Y. Tashkandi, L.C. Pavelka, M.A. Hanson, and K.M. Baines. Department of Chemistry, University of Western Ontario, London, ON N6A 5B7, Canada.

Corresponding author: Kim M. Baines (e-mail: kbaines2@uwo.ca).

This article is part of a Special Issue commemorating the 14th International Conference on the Coordination and Organometallic Chemistry of Germanium, Tin, and Lead (ICCOC-GTL 2013) held in Baddeck, NS, 2013.

Scheme 1.

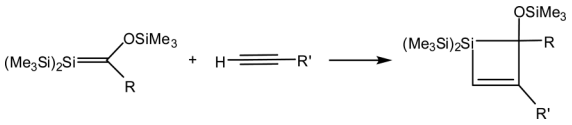

have also examined the addition of *trans*-(2-phenylcyclopropyl)-acetylene to germene **8**.

Results

Germene **8** was synthesized prior to each reaction and used in situ without purification. A pale yellow ethereal solution of fluorenylfluorodimesitylgermane, **9**, was cooled in a dry ice/acetone bath and then treated with *t*-BuLi. To avoid the formation of reduction products, less than 1 equiv. of *t*-BuLi was utilized, and thus, germene **8** was always contaminated with residual fluorogermane **9**. After warming the solution to room temperature, the colour of the solution changed from pale yellow to bright orange.[7] The orange solution of germene **8** is extremely air and moisture sensitive; the colour of the solution changes dramatically from bright orange to olive-green upon exposure to traces of moisture or oxygen. The presence of germene **8** was confirmed by ^{1}H nuclear magnetic resonance (NMR) spectroscopy before subsequent reactions. The germene was then dissolved in C_6D_6, diethyl ether, or tetrahydrofuran (THF), and excess alkyne was added. The reaction was kept at room temperature and monitored by ^{1}H NMR spectroscopy for up to 3 d. Germacyclohexene **10** was the only product formed from the reaction of germene **8** with phenylacetylene, 1-hexyne, or *trans*-(2-phenylcyclopropyl)acetylene (Scheme 5). The reactions of germene **8** with phenylacetylene or *trans*-(2-phenylcyclopropyl)acetylene were faster than that with 1-hexyne; the addition of phenylacetylene or *trans*-(2-phenylcyclopropyl) acetylene to **8** was complete within minutes, whereas the addition of 1-hexyne required approximately 24–72 h to go to completion. The products were isolated as yellow oils by preparative silica gel chromatography and were identified by ^{1}H, ^{13}C, ^{1}H–^{1}H–COSY (correlation spectroscopy), ^{13}C–^{1}H gHSQC (gradient heteronuclear single quantum coherence), and ^{13}C–^{1}H gHMBC (gradient heteronuclear multiple bond coherence) NMR and Fourier transform infrared (FT-IR) spectroscopy, electron impact mass spectrometry (EI-MS), and, in some cases, X-ray crystallography. Due to similarities between the spectroscopic data of **10a–10d**, only the data of **10a** will be discussed.

The high resolution mass spectral data of **10a** and the isotopic pattern of the signal assigned to the molecular ion were consistent with the molecular formula $GeC_{39}H_{36}$. The ^{1}H NMR spectral data of germacyclohexene **10a** were similar to those reported for the germaisoquinoline **11** formed upon the addition of benzonitrile to germene **8**[8] and oxagermin **12** produced in the addition of aldehyde **13** to germene **8** (Scheme 6).[9]

Broad singlets were observed at 1.64 and 2.32 ppm in the ^{1}H NMR spectrum of **10a** and were assigned to two ortho-methyl groups of nonequivalent mesityl substituents. A singlet at 4.65 ppm was observed and assigned to the Ge–$C_{(saturated)}H$ in the germacyclohexene ring. The chemical shift of this signal was in reasonable agreement with the chemical shifts of the analogous signals assigned to the Ge–CH in germaisoquinoline **11** (4.55 ppm)[8] and oxagermin **12** (4.62 ppm).[9] Integration of the signals assigned to the fluorenyl moiety did not correspond to the eight hydrogens present in the starting material; there was one hydrogen less than expected. The signal at 7.03 ppm in the ^{1}H NMR spectrum of **10a** was assigned to the vinylic hydrogen of the germacyclohexene ring. This signal correlated to the signal assigned to the ipso carbon of the phenyl substituent in the ^{13}C–^{1}H gHMBC spectrum of **10a**. All data are in agreement with the proposed structure of germacyclohexene **10a**. The addition of *trans*-(2-phenylcyclopropyl) acetylene to germene **8** yielded two diastereomers, **10c** and **10d**, in a ratio of 1:1. The coupling constants extracted from the multiplets of the two cyclopropyl spin systems showed maintenance of the original trans relationship between the cyclopropyl substituents. The regiochemistry of compounds **10a** and **10b** was confirmed by X-ray diffraction (Figs. 1 and 2, respectively), whereas the regiochemistry of **10c** and **10d** was assigned based on the known regiochemistry of **10a** and **10b**. The germacyclohexene ring is puckered in a half chair conformation (Figs. 1 and 2). All bond lengths and angles are within normal ranges. In contrast, no reaction was observed upon the addition of *t*-butylacetylene and trimethylsilylacetylene to germene **8**, even with gentle heating for 2 d.

The addition of ethoxyacetylene to germene **8** showed different reactivity. In this case, both the six-membered ring germacyclohexene **10e** and the four-membered ring germacyclobutene **14** are formed in the reaction (Scheme 7). The ratio of **10e** to **14** was 1:1 when the reaction was performed in Et_2O. This ratio changed to 1:3, respectively, when THF was employed as the solvent of the reaction. Germacyclohexene **10e** and germacyclobutene **14** were the only products of the reaction and they were identified as a mixture by ^{1}H NMR spectroscopy due to their sensitivity to moisture.

Germacyclobutene **14** hydrolyzes rapidly upon exposure to air, yielding germanol **15**, which then isomerizes to **16** upon adsorption to silica (Scheme 8). The highest mass signals in the mass spectra of **15** and **16** were observed at *m*/*z* 564.2078 and 564.2106, respectively, corresponding to a 1:1 adduct between ethoxyacetylene and germene **8** and one molecule of H_2O for each isomer. The ^{1}H NMR spectrum of **15** revealed a singlet at 4.54 ppm, which was assigned to the sp^3 C–*H* in the fluorenyl moiety; the absence of coupling is consistent with the regiochemistry assigned. A strong absorption at 3444 cm^{-1} in the IR spectrum of **16** was assigned to the hydroxyl group. The key to assigning the regiochemistry in **16** lies in the identification of the linker between the Mes_2GeOH and the fluorenyl moiety. Two signals were observed in the ^{13}C NMR spectrum of **16** at 159.30 and 119.73 ppm, characteristic of a vinyl ether moiety. Neither of these signals correlated to a signal in the ^{1}H NMR spectrum of **16** as was evident in the ^{13}C–^{1}H gHSQC spectrum of **16**. Furthermore, there were no signals in the ^{1}H NMR spectrum of **16** between 4 and 6 ppm indicating the absence of a vinylic-type hydrogen. A correlation was observed between the signals at 159.30 and 119.73 ppm in the ^{13}C NMR spectrum and the signal at 3.32 ppm in the ^{1}H NMR spectrum of **16**, which was assigned to the CH_2Ge moiety. Moreover, the signal at 3.32 ppm is a singlet and integrates for two hydrogens. If ethoxyacetylene had added to germene **8** with the opposite regiochemistry followed by hydrolysis (that is, to produce **17**), the corresponding signal would integrate for a single hydrogen and exhibit coupling to the vinylic hydrogen. Furthermore, if **17** were indeed the structure, the characteristic signals for the vinyl ether moiety would be absent. All data observed are completely consistent with the regiochemistry elucidated for **16**.

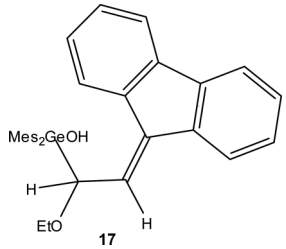

17

Germacyclohexene **10e** also hydrolyzes, presumably through the hemiacetal, to yield germacyclohexanone **18** at a slower rate (Scheme 9). The signal at the highest mass in the mass spectrum of **18** was observed at *m*/*z* 518.1668, which is consistent with the mass of a 1:1 adduct between ethoxyacetylene and germene **8**, with the

Scheme 2.

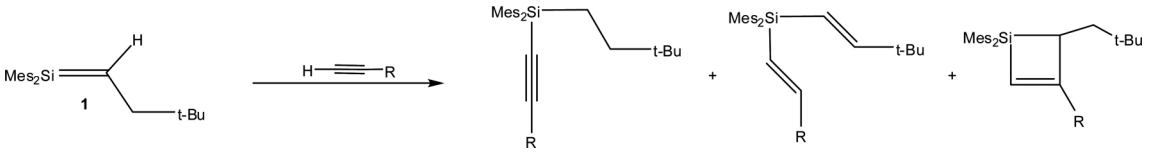

Scheme 3.

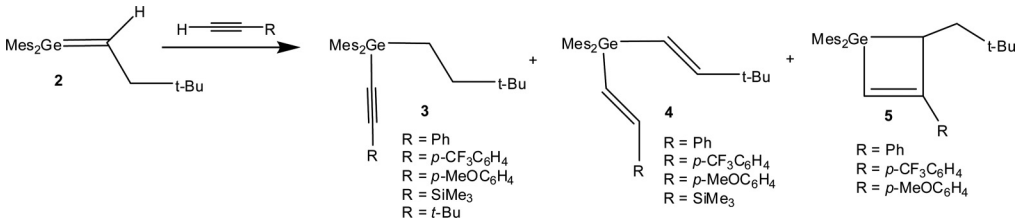

Scheme 4.

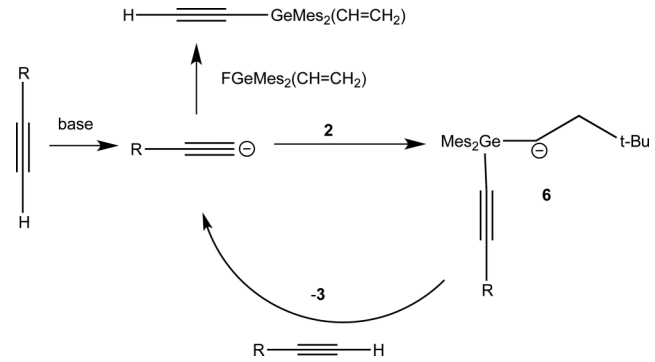

addition of H_2O and the loss of an ethoxy group. The presence of a carbonyl group was evident from the signal at 196.30 ppm in the ^{13}C NMR spectrum of **18**. The chemical shift of this signal is consistent with that reported for a typical β-germyl ketone (194.2 ppm).[10] The IR spectrum of **18** exhibits a strong absorption at 1664 cm^{-1}. The C=O moieties of related β-keto germanes absorb at approximately 1660 cm^{-1} (for example, Ph_3GeCH_2COPh at 1661 cm^{-1}), whereas the corresponding carbonyl moiety in α-keto germanes absorb at lower wavenumbers (for example, 1629 cm^{-1} for $Ph_3GeCOPh$).[11] The position of the IR absorption assigned to the carbonyl group in **18** supports the carbonyl moiety being in the β-position to Ge. The signal(s) assigned to the inequivalent CH_2 hydrogens, at 3.11 and 3.39 ppm, correlate to the signal at 196.30 ppm in the ^{13}C NMR spectrum of **18** assigned to the carbonyl group, to the signal assigned to one of the ipso-mesityl carbons, to the signal assigned to the Ge*C*H at 45.43 ppm, and to the unsaturated carbon on the opposite side of the carbonyl at 133.07 ppm. Given that the ^{13}C–^1H gHMBC spectroscopy experiment is optimized for three-bond correlations (8 Hz), the regiochemistry assigned is most consistent with the observed correlations. All these data unambiguously confirm the regiochemistry of germacyclohexanone **18**. Germacyclohexanone **18** was also synthesized by treatment of the product mixture containing **10e** with aqueous NH_4Cl in THF. Germacyclohexanone **18** is unstable and decomposes to unidentified products upon prolonged exposure to the ambient atmosphere.

Discussion

The addition of alkyl and aromatic terminal alkynes to germene **8** is clean and quantitative and produces germacyclohexenes **10a–10d**. As anticipated, there was no evidence for the formation of an ene adduct, which was attributed to the lack of an α-hydrogen in germene **8**. A product derived from insertion of the C–H of the terminal alkyne across the Ge=C of **8** was also not observed in any of the reactions. The absence of a C–H insertion product is attributed to the low basicity of the α-germyl anion derived from germene **8** (Scheme 10). The lack of a C–H insertion product supports the proposed chain mechanism for the formation of the C–H insertion adduct in the addition of terminal alkynes to germene **2**.[5]

The addition of *trans*-(2-phenylcyclopropyl)acetylene to germene **8** resulted in the formation of germacyclohexenes **10c** and **10d** with the cyclopropyl ring still intact, which rules out the presence of a cyclopropyl vinyl radical or cationic intermediate along the reaction pathway. Thus, the mechanism of the addition of alkynes to germene **8** is proposed to proceed via a concerted [2+4] cycloaddition where germene **8** acts as the diene (4π component) and the alkyne acts as the dienophile (2π component), followed by hydrogen transfer to give the corresponding germacyclohexene (Scheme 11). In all cases investigated, the proposed intermediate 1-germa-2,4-cyclohexadiene (Scheme 11) was not observed directly. The stereochemistry of the cyclopropyl ring in **10c** and **10d** remains trans; it does not scramble, which rules out the cyclopropyl ring opening and closing during the reaction. Analogous products were also observed in the addition of cyclopropylaldehyde **13** to germene **8**, which also resulted in the formation of oxagermin **12** with the cyclopropyl ring still intact.[9] *t*-Butylacetylene and trimethylsilylacetylene did not react with germene **8**, even after gentle heating for 2 d. Similarly, no cycloadduct was reported upon the addition of the same alkynes to neopentylsilene **1**[5] or neopentylgermene **2**.[6] The lack of reaction is attributed to the steric bulk of the substituents.

For a [2+4] cycloaddition reaction to take place, the diene must be in a cisoid conformation; the fluorenylidene substituent facilitates the coplanar cisoid conformation needed for the cycloaddition. A similar cycloaddition was observed in the addition of alkynes to *P*-mesityldiphenylmethylenephosphine (**19**; Scheme 12) even with the phenyl group not being held in a planar conformation.[12]

The regiochemistry of the addition of phenylacetylene and 1-hexyne to germene **8** was determined unambiguously from the X-ray structures of **10a** and **10b**, respectively, whereas the regiochemistry of the products derived from the addition of ethoxyacetylene to germene **8** was inferred from the structures elucidated for **16** and **18**. The regiochemistry of germacyclohexenes **10a–10e** is the same. Germacyclobutene **14**, formed by the addition of ethoxyacetylene to germene **8**, has the same relative regiochemistry as germacyclohexenes **10** and, in addition, the regiochemistry of **14** is consistent with that observed in the addition of alkynes to Brook silenes (Scheme 1)[2] and in the addition of aromatic alkynes to germene **2** to give germacyclobutenes **5** (Scheme 3).[6] In contrast, previous work in our group showed that the addition of ethoxyacetylene to germene **2** results in the for-

Scheme 5.

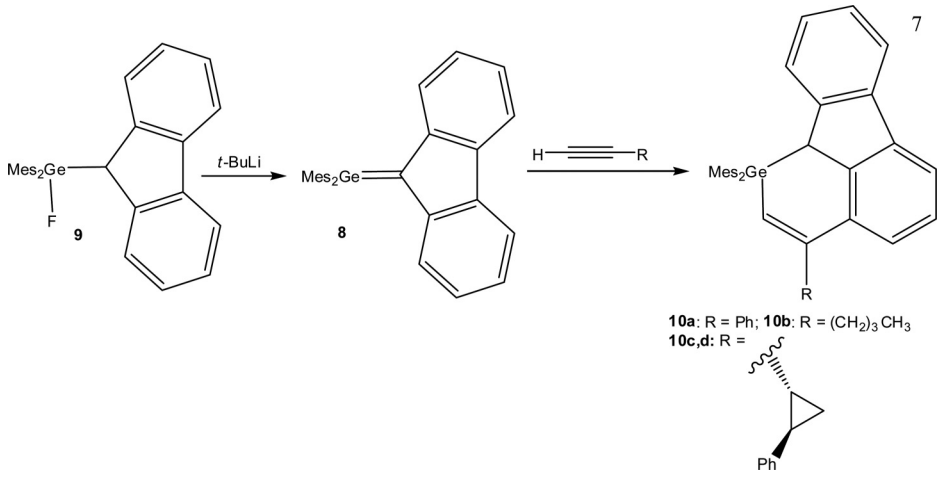

Scheme 6.

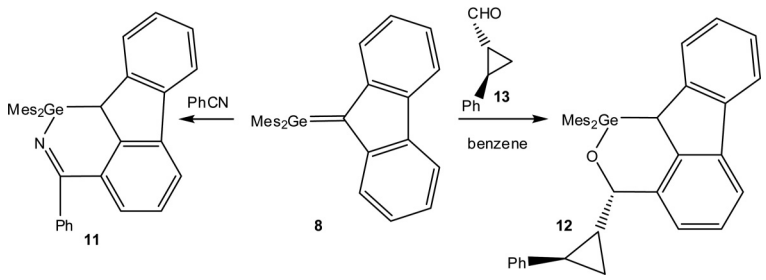

Fig. 1. Thermal ellipsoid plot of **10a** (30% probability surface). Selected bond lengths (Å) and angles (°): Ge–C1 = 1.994(3), Ge–C5 = 1.963(3), Ge–C31 = 1.971(3), Ge–C22 = 1.984(3), C1–C2 = 1.490(5), C2–C3 = 1.380(5), C3–C4 = 1.499(5), C4–C5 = 1.336(5); C5–Ge–C1 = 92.85(15), C2–C1–Ge = 107.5(2), C3–C2–C1 = 127.2(3), C2–C3–C4 = 120.5(3), C5–C4–C3 = 122.2(3), C4–C5–Ge = 122.0(3).

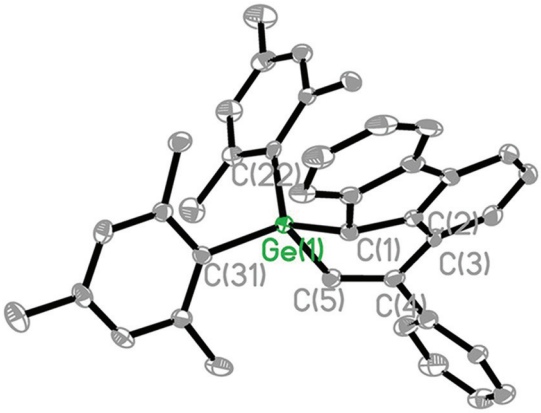

Fig. 2. Thermal ellipsoid plot of **10b** (30% probability surface). Selected bond lengths (Å) and angles (°): Ge–C19 = 1.924(2), Ge–C32 = 1.961(2), Ge–C1 = 1.961(2), Ge–C10 = 1.964(2), C32–C33 = 1.490(3), C33–C21 = 1.378(3), C20–C21 = 1.467(3), C19–C20 = 1.334(3); C20–C19–Ge = 123.75(18), C19–C20–C21 = 122.8(2), C33–C21–C20 = 121.3(2), C19–Ge–C32 = 94.40(10), C33–C32–Ge = 109.67(15), C21–C33–C32 = 127.6(2).

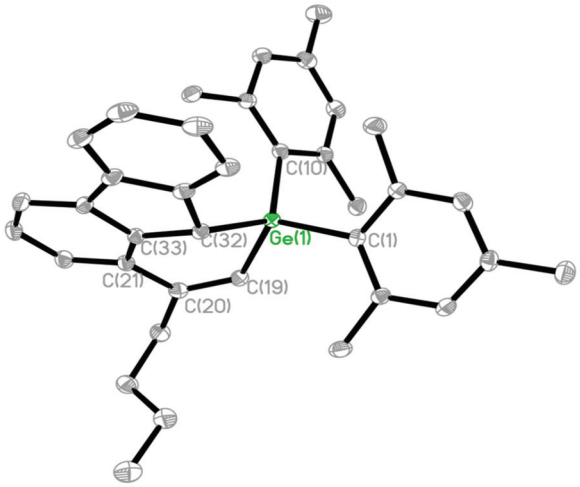

mation of germacyclobutene **20** (and vinylgermane **21**), which has the *opposite* regiochemistry compared to germacyclobutene **14**. Complexation between the alkyne and germene **2** was suggested to account for the unusual regiochemistry (Scheme 13).[6]

To gain more insight into the addition of alkynes to germenes and the regiochemistry of the reactions, density functional theory (DFT) calculations were performed at the TPSSTPSS/6-31G(d) level of theory. TPSSTPSS is a nonempirical meta-generalized gradient approximation (GGA) functional.[13] Meta-GGA functionals minimize the number of approximations used in the density functional. TPSSTPSS has been shown to give accurate results for a wide range of systems. In particular, we have found that it gives results for germanium systems, which are comparable to the popular B3LYP functional in a shorter amount of time.[14] Dimesitylfluorenylidenegermane **8** was modeled by 1-germabutadiene or 1,1-dimethylgermastyrene and acetylene was used to model 1-hexyne. All geometries were optimized at the TPSSTPSS/6-31G(d) level of theory.

Scheme 7.

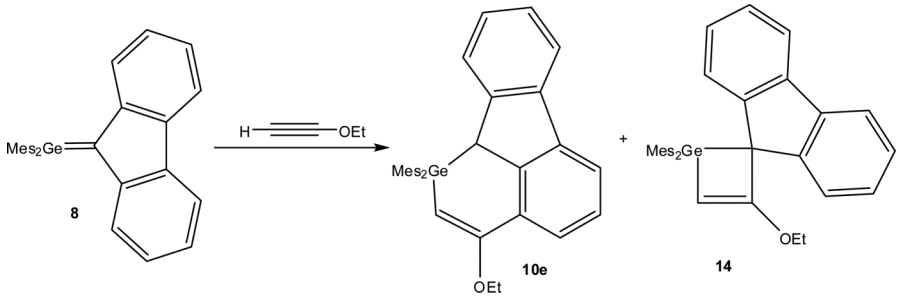

Scheme 8.

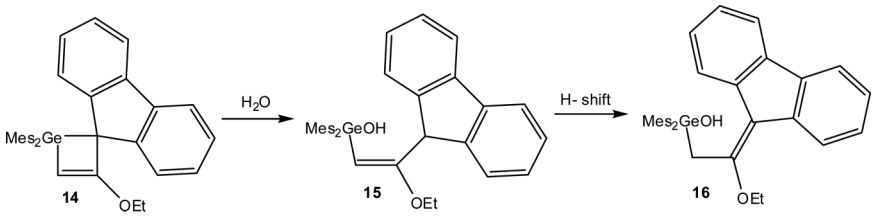

Scheme 9.

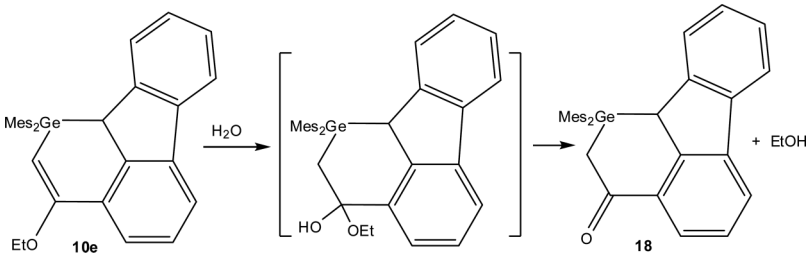

Scheme 10.

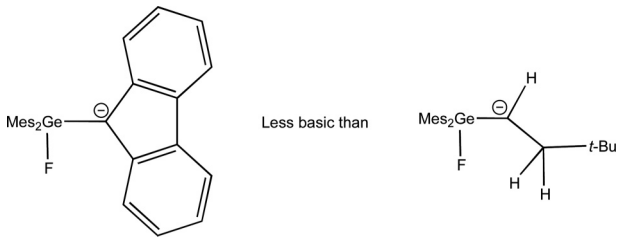

As was observed for R_2C=Ge(SiMe$_3$)(SiMe$_2$-*t*-Bu) (R_2C = adamantylidene),[15] the highest occupied molecular orbital and lowest unoccupied molecular orbital (HOMO–LUMO) energy gap of 1-germabutadiene (257 kJ/mol, 2.67 eV) was much less than in butadiene (399 kJ/mol, 4.14 eV; Table 1).

The HOMO and LUMO surfaces of butadiene, 1-germabutadiene, phenylacetylene, and ethoxyacetylene are show in Fig. 3. The largest orbital coefficient in the LUMO of 1-germabutadiene is located on the germanium atom (0.7633) and contributes 58% to the molecular orbital. In ethoxyacetylene, the largest orbital coefficient in the HOMO is located on the carbon bearing the hydrogen (0.7206, 52%) rather than the carbon bearing the ethoxy group (0.6933, 48%), which is consistent with the observed regiochemistry. In acetylene and phenylacetylene, the orbital coefficients on each carbon are equal. Since no difference in the frontier molecular orbital coefficients was observed in these cases, the observed regiochemistry is likely governed by minimization of steric interactions.

Two possibilities for the reaction pathway were considered: the HOMO of the conjugated germene, as modelled by 1,1-dimethylgermastyrene, interacting with the LUMO of the alkyne, known as a normal demand Diels–Alder reaction, or the LUMO of the conjugated germene interacting with the HOMO of the alkyne, known as an inverse demand Diels–Alder reaction. In the case of phenylacetylene, the calculated differences between the energy levels for both the HOMO of the germastyrene and the LUMO of the alkyne and the HOMO of the alkyne and the LUMO of the germastyrene are the same at 328 kJ/mol (3.40 eV; Table 2). However, when ethoxyacetylene or acetylene is the alkyne, the calculated energy differences between the LUMO of germastyrene and the HOMO of the alkyne are much smaller than the calculated differences for the opposite combinations (Table 2). Thus, we believe these reactions are best classified as inverse demand Diels–Alder reactions. In general, inverse demand Diels–Alder reactions are favoured when a dienophile with electron-donating substituents reacts with a diene. The electron-donating groups on the dienophile raise the energy of the HOMO, which decreases the energy difference between the HOMO of the dienophile and the LUMO of the diene, and thus, accelerates the rate of the reaction. Phenylacetylene, *trans*-(2-phenylcyclopropyl)acetylene, and ethoxyacetylene are conjugated alkynes with electron-donating groups and the addition of these alkynes to germene **8** was complete within a few minutes, whereas the addition of 1-hexyne to germene **8** took several days to go to completion. Correspondingly, the energy gap between the LUMO of 1,1-dimethylgermastyrene and the HOMO of acetylene (440 kJ/mol, 4.54 eV) decreases significantly to 303 kJ/mol (3.13 eV) when the alkyne is changed to ethoxyacetylene and to 328 kJ/mol (3.40 eV) when it is changed to phenylacetylene (Table 2), which is in agreement with the qualitative assessment of the reaction kinetics. Thus, the formation of germacyclohexenes **10a–10d** follows the trends established for carbon chemistry. However, even though

Scheme 11.

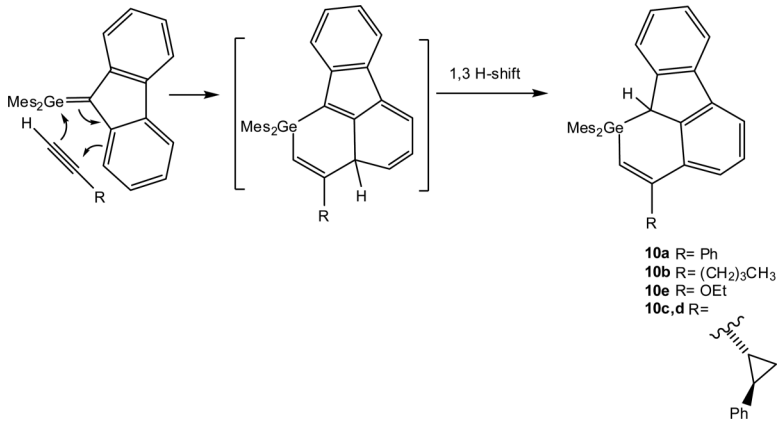

Scheme 12.

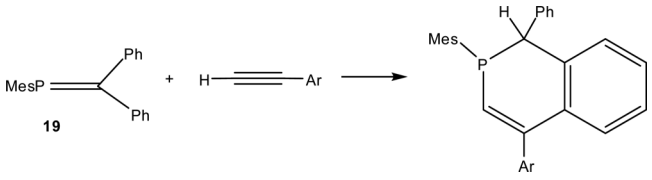

Scheme 13.

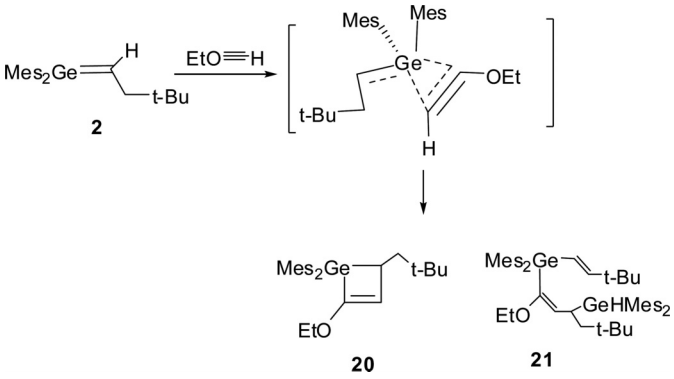

Table 1. HOMO and LUMO energies (hartree) and energy differences between the HOMO and the LUMO (kJ/mol) for various germenes and alkynes.

Compound	HOMO	LUMO	HOMO–LUMO gap
1-Germabutadiene	−0.176	−0.078	257
Butadiene	−0.199	−0.047	399
Acetylene	−0.245	0.024	706
Ethoxyacetylene	−0.193	0.038	606
Phenylacetylene	−0.203	−0.051	399
1,1-Dimethylgermastyrene	−0.154	−0.056	257

the reaction of 1-hexyne with germene **8** took longer to go to completion compared to the conjugated alkynes, the reaction proceeds much faster than the analogous all-carbon systems. In comparison, the addition of nonactivated alkynes to dienes requires high temperature and (or) the presence of a catalyst to proceed at a reasonable rate.[16]

The substituent in ethoxyacetylene is strongly electron donating. In this case, both the dienophile (ethoxyacetylene) and the diene (germene **8**) are electron rich species. The mismatch in electron demand presumably slows the rate of the Diels–Alder reaction and allows for the competitive formation of another cycloadduct. The mechanism for the formation of germacyclobutene

Fig. 3. Highest occupied and lowest unoccupied molecular orbitals of (A) butadiene, (B) 1-germabutadiene, (C) phenylacetylene, and (D) ethoxyacetylene. All molecular orbitals were calculated at the TPSSTPSS/6-31G(d) level.

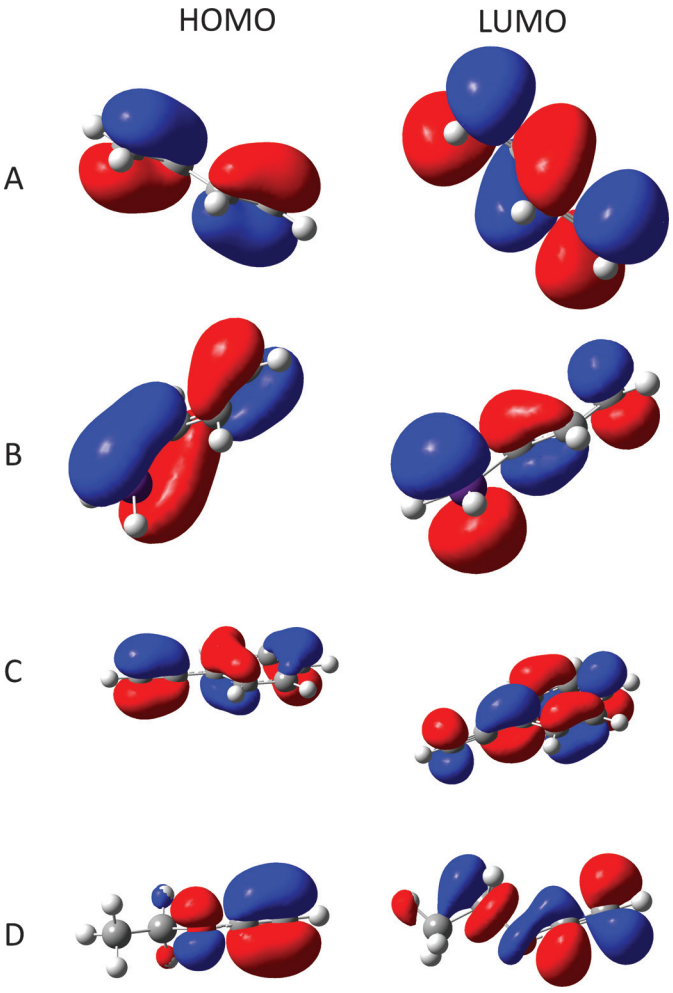

14 is likely stepwise, where the nucleophile (ethoxyacetylene) attacks germene **8** to give a zwitterionic intermediate, followed by cyclization (Scheme 14). This is in contrast to the formation of germacyclobutene **20**, from the addition of ethoxyacetylene to germene **2**, which has the opposite regiochemistry and was proposed to proceed via complexation (Scheme 13). Furthermore, the zwitterionic intermediate proposed from the nucleophilic addi-

Table 2. Magnitude of the HOMO–LUMO gaps (kJ/mol) for 1,1-dimethylgermastyrene and various alkynes.

Alkyne	Germene HOMO–alkyne LUMO gap	Alkyne HOMO–germene LUMO gap
Phenylacetylene	328	328
Acetylene	525	440
Ethoxyacetylene	562	303

Scheme 14.

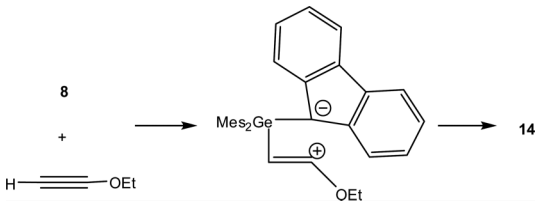

tion of ethoxyacetylene to germene **8** (Scheme 14) would be stabilized due to the delocalization of the negative charge over the fluorenyl group[17] and the positive charge can be stabilized by the ethoxy group. The observed increase in the ratio of the germacyclobutene **14** over germacyclohexene **10e** when the reaction is carried out in THF rather than in diethyl ether also supports our proposed stepwise, zwitterionic cycloaddition mechanism, as the solvent (THF) with the greater dielectric constant can stabilize the zwitterionic intermediate and lead to an increase in the rate of germacyclobutene **14** formation. Thus, the difference in regiochemistry between the addition of ethoxyacetylene to germenes **2** and **8** may be a consequence of the relative ability of the germenic carbon to accommodate a negative charge.

In summary, our hypothesis that the reaction of germene **8** with alkynes would indeed be simpler than the reactions of germene **2** because of the lack of an α-hydrogen and the reduced basicity of the conjugate base of **8** proved to be correct. The addition reactions of alkynes to germene **8** are clean; they undergo cycloaddition exclusively. As in carbon chemistry, a [4+2] cycloaddition pathway is favoured over a [2+2] cycloaddition pathway unless an extremely electron-rich alkyne is utilized. Rearrangement of the cyclopropyl ring did not occur during the addition of the alkynyl mechanistic probe, *trans*-(2-phenylcyclopropyl)-acetylene, to germene **8**, which rules out the presence of a radical or cationic intermediate along the reaction pathway. Thus, the formation of germacyclohexenes **10a–10e** is proposed to occur via a concerted [2+4] cycloaddition followed by hydrogen transfer. The addition of ethoxyacetylene to germene **8** produced germacyclobutene **14** and germacyclohexene **10e**, where **14** is likely formed via a stepwise [2+2] cycloaddition through a zwitterionic intermediate. The difference in reaction rate between aromatic and aliphatic alkynes toward germene **8** reveals that conjugated germenes mimic carbon-based dienes in terms of their cycloaddition chemistry. We continue to investigate the cycloaddition reactions of germenes with the goal of understanding their reactivity more completely.

Experimental

DFT calculations

First principles calculations were performed using Gaussian 09[18] on the Shared Hierarchical Academic Research Computing Network (SHARCNET, www.sharcnet.ca). Calculations were performed on an 8 core Xeon 2.83 GHz CPU with 16 GB memory. All calculations were performed at the TPSSTPSS[13]/6-31G(d) level of theory. Molecular orbitals were calculated using NBO version 3. Cube files were generated using the cubegen utility and visualized in GaussView 3.09.

General experimental details

All manipulations were performed in flame-dried Schlenk tubes, or NMR tubes sealed with a septum, under an inert atmosphere of argon. Benzene-d_6 was distilled from $LiAlH_4$, stored over 4 Å molecular sieves, and degassed prior to use. *t*-BuLi was purchased from Sigma-Aldrich. The NMR standards used were residual C_6D_5H (7.15 ppm) for ^1H NMR spectra, C_6D_6 central transition (128.00 ppm) for ^{13}C NMR spectra, residual $CHCl_3$ (7.26 ppm) for ^1H NMR spectra, and $CDCl_3$ central transition (77.00 ppm) for ^{13}C NMR spectra. IR spectra were recorded (cm^{-1}) from thin films on a Bruker Tensor 27 FT-IR spectrometer. Electron impact mass spectra were obtained using a MAT model 8400 mass spectrometer using an ionizing voltage of 70 eV. Mass spectral data are reported in mass-to-charge units, *m*/*z*. *Trans*-(2-phenylcyclopropyl)acetylene was synthesized as follows: reduction of *trans*-(2-phenylcyclopropyl)-carboxylic acid using excess $LiAlH_4$ produced the corresponding alcohol, which was oxidized under Swern conditions. The resulting aldehyde was converted to the dibromoolefin and then to *trans*-(2-phenylcyclopropyl)acetylene using Corey–Fuchs conditions. The product was identified by comparison of the ^1H NMR data to those in the literature.[6] A modified route to synthesize fluorenylfluorodimesitylgermane (**9**) was developed due to the complexity of the purification step in the reported procedure.[9] Hydrolysis using an NaOH solution of chlorofluorenyldimesitylgermane to give the hydroxy analog followed by fluorination using HF gave **9**. The overall yield (40%) is comparable to the yield from the original route (41%).[9]

General procedure for the reaction of alkynes with germene 8

A solution of fluorenylfluorodimesitylgermane (50 mg, 0.1 mmol) dissolved in diethyl ether (3 mL) was cooled to –78 °C. *t*-BuLi (0.06 mL, 1.7 mol/L in pentane, 0.1 mmol) was added slowly. The colour of the solution changed from pale yellow to bright orange. The reaction mixture was allowed to stir at room temperature for 2 h. An aliquot was analyzed by ^1H NMR spectroscopy (C_6D_6) and was found to contain germene **8** (~88%). The ether was removed in vacuo (if required), yielding a bright orange residue, and the residue was dissolved in C_6D_6 (1.1 mL). Alkyne (1.2 equiv.) was added directly to the germene solution. The progress of the reaction was monitored by ^1H NMR spectroscopy for up to 3 d. The solvent was removed by rotary evaporation yielding a yellow residue. The ratio of products in the crude reaction mixture was determined by ^1H NMR spectroscopy. The product mixture was contaminated with residual alkyne and unreacted fluorogermane **9**. The products were separated from fluorogermane **9** and residual alkyne by preparative thin layer chromatography on silica gel (hexanes and dichloromethane, 50:50) followed by second preparative thin layer chromatography on silica gel (hexanes) yielding yellow oil (mixed with a colourless solid in the case of **10a** and **10b**), **10a–10d** (43%–45%).

10a

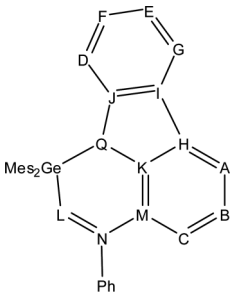

10a

IR (thin film, cm^{-1}): 2922 (s), 2851 (s), 1731 (m), 1603 (m), 1449 (s), 1377 (m), 1264 (m), 1028 (m), 847 (m), 810 (m), 740 (m). ^1H NMR ($CDCl_3$, 600 MHz) δ: 7.89 (d, 1H, G, *J* = 7.8 Hz), 7.76 (d, 1H, A, *J* =

7.8 Hz), 7.44–7.32 (m, 6H, Ph-H and F), 7.32–7.28 (m, 1H, D), 7.27–7.22 (m, 2H, B and E), 7.03 (s, 1H, L), 6.93 (d, 1H, C, J = 7.2 Hz), 6.91 (s, 2H, *m*-Mes H), 6.55 (s, 2H, *m*-Mes-H), 4.65 (s, 1H, Q), 2.32 (br s, 9H, *o*,*p*-Mes), 2.11 (s, 3H, *p*-Mes), 1.64 (br s, 6H, *o*-Mes). ^{13}C NMR ($CDCl_3$, 100 Hz) δ: 150.92 (N), 145.80 (J), 143.81 (*i*-Ph), 143.24 (*o*-Mes), 142.98 (K), 141.56 (I), 141.53 (*o*-Mes), 140.37 (H), 138.51 (*p*-Mes), 138.07 (*p*-Mes), 137.71 (*i*-Mes), 134.81 (*i*-Mes), 134.06 (M), 132.91 (L), 129.40 (*m*-Mes), 128.67 (*o*-Ph), 128.26 (*m*-Mes), 128.10 (*m*-Ph), 127.33 (*p*-Ph), 126.60 (C), 126.37 (E), 126.12 (B), 125.76 (F), 124.35 (D), 120.16 (G), 119.27 (A), 41.88 (GeCH), 25.56 (br s, *o*-Mes), 22.71 (*o*-Mes), 21.03 (*p*-Mes), 20.80 (*p*-Mes). High-resolution EI-MS for $C_{39}H_{36}{}^{70}Ge$ (*m*/*z*), calcd.: 574.206; found: 574.204.

10b

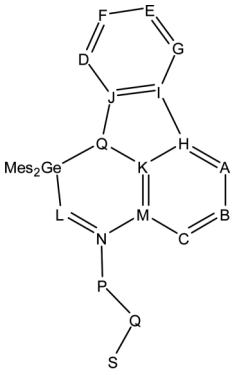

10b

^{1}H NMR ($CDCl_3$, 600 MHz) δ: 7.86 (d, 1H, D, J = 7.8 Hz), 7.74 (d, 1H, A, J = 7.8 Hz), 7.37–7.31 (m, 4H, B, G, and C), 7.23–7.19 (m, 2H, F and E), 6.91 (s, 2H, *m*-Mes-H), 6.79 (s, 1H, L), 6.51 (s, 1H, *m*-Mes-H), 4.45 (s, 1H, L), 2.87 (dt, 1H, P, J = 7.8, 14.4 Hz), 2.53 (dt, 1H, P, J = 7.8, 14.9 Hz), 2.32 (s, 9H, *o*,*p*-Mes), 2.08 (s, 3H, *p*-Mes), 1.63–1.57 (m, 8H, *o*-Mes and Q), 1.4 (m, 2H, R), 0.93 (t, 3H, S, J = 7.2 Hz). ^{13}C NMR ($CDCl_3$, 150 Hz) δ: 149.07 (N), 145.96 (K), 143.22 (bs, *o*-Mes), 142.73 (I), 141.57 (J), 141.38 (*o*-Mes), 140.36 (H), 138.38 (*p*-Mes), 138.21 (*i*-Mes), 137.96 (*p*-Mes), 135.27 (*i*-Mes), 133.80 (M), 129.34 (*m*-Mes), 129.00 (L), 128.17 (*m*-Mes), 126.25 (B), 126.23 (F), 125.61 (E), 124.23 (D), 123.30 (C), 120.04 (G), 118.87 (A), 42.00 (Ge-*C*H), 37.21 (P), 30.48 (Q), 25.5 (br s, *o*-Mes), 22.60 (*o*-Mes), 22.50 (R), 21.05 (*p*-Mes), 20.78 (*p*-Mes), 14.02(S). High-resolution EI-MS for $C_{37}H_{40}{}^{70}Ge$ (*m*/*z*), calcd.: 554.2373; found: 554.2369. Anal. calcd. for $C_{37}H_{40}{}^{70}Ge$: C 79.73, H 7.23; found: C 75.36, H 7.13.

10c and 10d

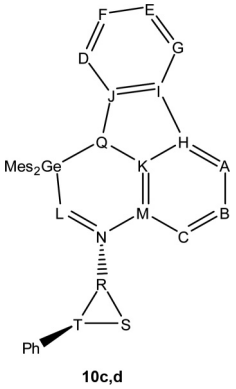

10c,d

Mixture of diastereomers, a colourless solid contaminated with $[Mes_2Ge(fluorenyl)]_2O$[7] (1:1:0.13) and other minor impurities. ^{1}H NMR (C_6D_6, 600 MHz) δ: 7.79 (d, 1H, G, J = 7.8 Hz), 7.78 (d, 1H, G, J = 7.8 Hz), 7.67 (d, 1H, A, J = 7.8 Hz), 7.62 (d, 1H, A, J = 7.8 Hz), 7.57 (d, 1H, C, J = 7.8 Hz), 7.52 (d, 1H, C, J = 7.2 Hz), 7.50 (d, 2H, 2D, J = 7.2 Hz), 7.25 (m (2× td), 2H, 2E), 7.21 (t, 1H, B, J = 7.2 Hz), 7.16–7.14 (m, B + F + Ph), 7.12 (t, F, J = 7.8 Hz), 7.07–7.02 (m, 5H, Ph), 6.99 (d, 1H, L, J = 1 Hz), 6.92 (s, 1H, L), 6.86 (m, 1H, Ph), 6.85 (s, 4H, *m*-Mes2), 6.41 (s, 2H, *m*-Mes1), 6.39 (s, 2H, *m*-Mes1), 4.64 (s, 1H, Q), 4.54 (s, 1H, Q), 2.46 (s, 6H, *o*-Mes2), 2.43 (s, 6H, *o*-Mes2), 2.24–2.20 (m, T′), 2.18, 2.17 (s each, 6H total, *p*-Mes2), 2.15–2.10 (m, T), 2.08–2.02 (m, R′), 1.87 (s, 3H, *p*-Mes1), 1.85 (s, 3H, *p*-Mes1), 1.80 (br s, 12H, *o*-Mes1), 1.80–1.77 (m, R), 1.49 (ddd, 1H, S1, J = 5.4, 6.3, 9.6 Hz), 1.26 (ddd, 1H, S′, J = 4.8, 6.3, 9.0 Hz), 1.18 (ddd, 1H, S′, J = 4.8, 6.6, 9.0 Hz), 1.07 (ddd, 1H, S1, J = 4.8, 5.4, 8.4 Hz). ^{13}C NMR (C_6D_6, 150 Hz) δ: 149.43 (N), 149.34 (N), 146.42 (J), 146.56 (J), 143.62 (*o*-Mes2), 143.53 (*o*-Mes2), 143.20 (Ph), 143.16 (K), 143.07 (Ph), 142.94 (K), 142.35 (I), 142.31 (I), 141.61 (*o*-Mes1), 141.58 (*o*-Mes1), 140.93 (2H), 138.88 (*p*-Mes2), 138.35 (*p*-Mes1), 138.29 (*i*-Mes1), 138.09 (*i*-Mes1), 135.76 (*i*-Mes2), 135.66 (*i*-Mes2), 135.12 (M), 135.05 (M), 130.11 (*m*-Mes2), 129.09 (*m*-Mes1), 129.05 (*m*-Mes1), 128.89 (L), 127.15 (B), 127.05 (B), 126.94 (F), 126.92 (F), 126.50 (2E), 126.37 (Ph), 126.35 (Ph), 126.31 (L), 126.30 (Ph), 126.17 (Ph), 126.14 (Ph), 126.04 (Ph), 124.75 (D), 124.71 (D), 124.65 (C), 124.63 (C), 120.79 (G), 119.90 (A and G), 119.76 (A), 42.58 (Q), 42.52 (Q), 30.41 (T), 29.79 (T′), 28.19 (R′), 25.93 (*o*-Mes2), 25.85 (*o*-Mes2), 24.53 (R), 23.21 (*o*-Mes1), 21.23 (*p*-Mes2), 20.89 (*p*-Mes1), 20.71 (*p*-Mes1), 17.96 (S′), 14.64 (S). High-resolution EI-MS for $C_{42}H_{40}{}^{70}Ge$ *m*/*z*, calcd.: 614.2372; found: 614.2373. (Primes or numbers indicate the signals belong to the same diastereomer.)

Addition of ethoxyacetylene to germene 8

A solution of fluorogermane **9** (50 mg, 0.1 mmol) dissolved in diethyl ether (3 mL) was cooled to –78 °C. *t*-BuLi (0.06 mL, 1.7 mol/L in pentane, 0.1 mmol) was added slowly. The colour of the solution changed from pale yellow to bright orange. The reaction mixture was allowed to stir at room temperature for 2 h. An aliquot was analyzed by ^{1}H NMR spectroscopy (C_6D_6) and was found to contain germene **8** (~88%). The ether was removed in vacuo (if required), yielding a bright orange residue. The residue was dissolved in one of three solvents: C_6D_6, diethyl ether, or THF (1.1 mL). Ethoxyacetylene (1.2 equiv.) was added directly to the germene solution. The solvent was removed by rotary evaporation yielding a yellow residue. The ratio of products (**10e**:**14**) in the crude reaction mixture was determined by ^{1}H NMR spectroscopy. The product mixture was contaminated with residual alkyne and unreacted fluorogermane **9**. The mixture was separated by preparative thin layer chromatography on silica gel (hexanes and dichloromethane, 50:50) to give contaminated samples of **10e** and **14**. Further attempts at purification by chromatography resulted in the hydrolysis of **10e** and **14**; compounds **15**, **16**, and **18** were isolated from the plate. Compound **15** underwent isomerization to **16** in solution. A third attempt to purify compounds **16** and **18** by preparative thin layer chromatography on silica gel (hexanes) gave **16** in acceptable purity, however, **18** was contaminated with $Mes_2GeOHCHR_2$.[7]

10e

Yellow oil contaminated with fluorene and other impurities (1:0.8). ^{1}H NMR (C_6D_6, 600 MHz) δ: 7.96 (d, 1H, J = 7.2 Hz), 7.78 (d, 1H, J = 7.8 Hz), 7.71 (d, 1H, J = 7.8 Hz), 7.51 (d, 1H, J = 7.2 Hz), 7.35 (t, 1H, J = 7.2 Hz), ~7.23 (m; all for fluorenyl-H), 6.85 (s, 2H, *m*-Mes), 6.44 (s, 2H, *m*-Mes), 5.58 (s, 1H, vinyl H), 4.58 (s, 1H, Ge-C*H*), 3.70 (dq, 1H, OCH, J = 16.8, 6 Hz), 3.52 (dq, 1H, OCH, J = 16.2, 6.6 Hz), 2.47 (br s, 6H, *o*-Mes), 2.18 (s, 3H, *p*-Mes), 1.90 (s, 3H, *p*-Mes), 1.80 (br s, 6H, *o*-Mes), 1.15 (t, 3H, CH_3, J = 6.6 Hz).

14

Yellow oil. ^{1}H NMR (C_6D_6, 600 MHz) δ: 7.68 (d, 2H, J = 7.2 Hz), 7.29 (d, 2H, J = 7.8 Hz), 7.16 (t, 2H, J = 7.8 Hz), 7.00 (t, 2H, J = 7.2 Hz; all for fluorenyl-H), 6.66 (s, 4H, *m*-Mes), 5.48 (s, 1H, vinyl H), 3.56 (q, 2H, OCH_2 J = 7.2 Hz), 2.12 (br s, 12H, *o*-Mes), 2.06 (s, 6H, *p* Mes), 0.74 (t, 3H, CH_3, J = 6.6 Hz).

15

Yellow oil. ^{1}H NMR (C_6D_6, 400 MHz) δ: 7.58–7.54 (m, 2H), 7.2 (m, 6H; all fluorenyl-H), 6.72 (s, 4H, *m*-Mes), 5.25 (s,1H, vinyl), 4.54 (s,1H, CHR_2), 3.09 (q, 2H, J = 7.2 Hz, OCH_2), 2.56 (s, 12H, *o*-Mes), 2.08 (s, 6H, *p*-Mes), 0.49 (t, 3H, J = 7.2 Hz, OCH_2CH_3). High-resolution EI-MS for $C_{35}H_{38}O_2{}^{74}Ge$ *m*/*z*, calcd.: 564.2088; found: 564.2078.

16

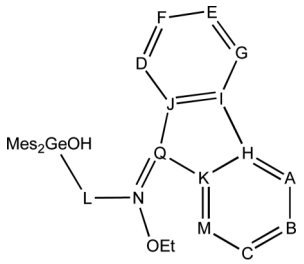

16

Yellow oil. IR (thin film, cm^{-1}): 3444 (br s), 2923 (m), 1612 (w), 1734 (w), 1602 (w), 1303 (s), 1025 (w), 758 (s). ^{1}H NMR (C_6D_6, 400 MHz) δ: 8.54 (dt, 1H, M, J = 7.8, 0.8 Hz), 7.86 (d, 1H, G, J = 7.6 Hz), 7.72 (dt, 1H, A, J = 7.8, 0.8 Hz), 7.68 (ddd, 1H, D, J = 6.8, 1.2, 0.8 Hz), 7.39 (td, 1H, C, J = 7.8, 1.2 Hz), 7.27 (td, 1H, B, J = 7.6, 1.2 Hz), 7.12 (td, 1H, F, J = 7.6, 1.2 Hz), 7.07 (td, 1H, E, J = 7.2, 1.6 Hz), 6.60 (s, 4H, *m*-Mes), 3.50 (q, 2H, O-CH_2, J = 6.8 Hz), 3.32 (s, 2H, L), 2.37 (s, 12H, *o*-Mes), 2.03 (s, 6H, *p*-Mes), 0.92 (t, 3H, CH_3, J = 7.2 Hz). ^{13}C NMR (C_6D_6, 100 Hz) δ: 159.30 (N), 143.01 (*o*-Mes), 139.97 (J), 139.38 (*p*-Mes), 139.01 (K), 138.22 (H), 138.11 (I), 136.09 (*i*-Mes), 129.83 (*m*-Mes), 127.50 (C), 126.67 (E), 126.40 (B), 126.21 (M), 125.89 (F), 123.30 (G), 120.27 (D), 119.73 (Q), 119.65 (A), 64.63 (OCH_2), 27.83 (L), 23.85 (*o*-Mes), 21.16 (*p*-Mes), 15.02 (CH_3). High-resolution EI-MS for $C_{35}H_{38}O_2{}^{74}Ge$ *m*/*z*, calcd.: 564.2088; found: 564.2106.

18

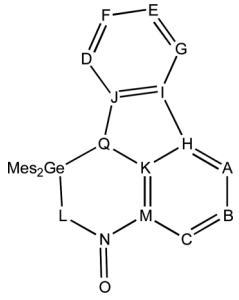

18

Yellow oil contaminated with $Mes_2GeOHCHR_2$[7] in a 1:0.5 ratio. IR (thin film, cm^{-1}): 2919 (m), 2849 (m), 1665 (s), 1601 (m), 1448 (s), 1415 (m), 1414 (m), 1276 (m), 1261 (m), 1025 (s), 849 (m), 795 (s), 765 (m), 737 (s). ^{1}H NMR (C_6D_6, 600 MHz) δ: 8.2 (d, 1H, C, J = 7.8 Hz), 7.71 (d, 1H, G, J = 7.2 Hz), 7.70 (d, 1H, A, J = 6.6 Hz), 7.34 (d, 1H, D, J = 7.8 Hz), 7.18 (t, 1H, B, J = 7.2 Hz), ~7.22 (E, overlap with signal from the germol), 7.11 (t, 1H, F, J = 7.8 Hz), 6.74 (s, 2H, *m*-Mes2), 6.35 (s, 2H, *m*-Mes2), 4.23 (s, 1H, Q), 3.39 (d, 1H, L, J = 12 Hz), 3.11 (d, 1H, L, J = 12 Hz), 2.20 (s, 6H, *o*-Mes2), 2.10 (s, 3H, *p*-Mes2), 1.82 (s, 3H, *p*-Mes1), 1.60 (s, 6H, *o*-Mes1). ^{13}C NMR (C_6D_6, 100 Hz) δ: 196.30 (N), 147.98 (K), 145.59 (J), 143.04 (*o*-Mes1), 142.05 (*o*-Mes2),141.81 (H), 141.37 (I), 139.47 (*p*-Mes2), 138.78 (*p*-Mes1), 134.99 (*i*-Mes2), 133.48 (*i*-Mes1), 133.07 (M), 130.03 (*m*-Mes2), 129.27 (*m*-Mes1), 127.34 (F), 127.04 (B), 126.55 (E), 126.38 (C), 124.55 (D), 124.18 (A), 120.61 (G), 45.43 (Q), 42.74 (L), 24.70 (*o*-Mes2), 22.43 (*o*-Mes1), 20.98 (*p*-Mes2), 20.70 (*p*-Mes1). High-resolution EI-MS for $C_{33}H_{32}O^{74}Ge$ *m*/*z*, calcd.: 518.1642; found: 518.1668.

Supplementary data

Supplementary data (figures containing NMR spectra for all new compounds, details of the X-ray structure determinations of **10a** and **10b** and tables summarizing the computational data) are available with the article through the journal Web site at http://nrcresearchpress.com/doi/suppl/10.1139/cjc-2013-0532. CCDC 960004 and 960005 contain the X-ray data in CIF format for this manuscript. These data can be obtained, free of charge, via http://www.ccdc.cam.ac.uk/products/csd/request (Or from the Cambridge Crystallographic Data Centre, 12 Union Road, Cambridge CB2 1E2, UK; fax: +44 1223 33603; or e-mail: deposit@ccdc.cam.ac.uk).

Acknowledgements

Computational work was made possible by the facilities of the Shared Hierarchical Academic Research Computing Network (SHARCNET; www.sharcnet.ca) and Compute/Calcul Canada. We thank the Natural Sciences and Engineering Research Council of Canada (NSERC) and the University of Western Ontario for financial support, King Abdul Aziz University (Saudi Arabia) for a scholarship to N.Y.T., and Aneta Borecki for the X-ray structure determination of **10b**.

References

(1) Ottosson, H.; Steel, P. G. *Chem. Eur. J.* **2006**, *12*, 1576. doi:10.1002/chem.200500429.
(2) (a) Brook, A. G.; Harris, J. W.; Lennon, J.; El Sheikh, M. *J. Am. Chem. Soc.* **1979**, *101*, 83. doi:10.1021/ja00495a015; (b) Brook, A. G.; Baumegger, A.; Lough, A. I. *Organometallics* **1992**, *11*, 3088. doi:10.1021/om00045a024.
(3) Gottschling, S. E.; Grant, T. N.; Milnes, K. K.; Jennings, M. C.; Baines, K. M. *J. Org. Chem.* **2005**, *70*, 2686. doi:10.1021/jo047797n.
(4) Milnes, K. K.; Jennings, M. C.; Baines, K. M. *J. Am. Chem. Soc.* **2006**, *128*, 2491. doi:10.1021/ja057596g.
(5) Milnes, K. K.; Pavelka, L. C.; Baines, K. M. *Organometallics* **2010**, *29*, 5972. doi:10.1021/om100756p.
(6) Pavelka, L. C.; Baines, K. M. *Organometallics* **2011**, *30*, 2261. doi:10.1021/om200048p.
(7) Couret, C.; Escudie, J.; Stage, J.; Lazraq, M. *J. Am. Chem. Soc.* **1987**, *27*, 828. doi:10.1021/ja00248a056.
(8) El Kettani, S. A.; Lazraq, M.; Ranaivonjatovo, H.; Escudie, J.; Couret, C.; Gornitzka, H.; Merceron, N. *Organometallics* **2004**, *23*, 5062. doi:10.1021/om0494622.
(9) Allan, C. J.; Reinhold, C.; Pavelka, L. C.; Baines, K. M. *Organometallics* **2011**, *30*, 3010. doi:10.1021/om200114n.
(10) Liang, Y.; Pitteloud, J.-P.; Wnuk, S. F. *J. Org. Chem.* **2013**, *78*, 5761. doi:10.1021/jo400590z.
(11) Brook, A. G. *Adv. Organomet. Chem.* **1968**, *7*, 95. doi:10.1016/S0065-3055(08)60293-2.
(12) Pavelka, L. C.; Baines, K. M. *Dalton Trans.* **2012**, *41*, 3294. doi:10.1039/c2dt11690a.
(13) Tao, J.; Perdew, J. P.; Staroverov, V. N.; Scuseria, G. E. *Phys. Rev. Lett.* **2003**, *91*, 146401. doi:10.1103/PhysRevLett.91.146401.
(14) Hanson, M. A.; Sutrisno, A.; Terskikh, V. V.; Baines, K. M.; Huang, Y. *Chem. Eur. J.* **2012**, *18*, 13770. doi:10.1002/chem.201201944.
(15) Li, B.-Y.; Su, M.-D. *Organometallics* **2011**, *30*, 6189.
(16) Tonogaki, K.; Mori, M. *Tetrahedron Lett.* **2002**, *43*, 2235. doi:10.1016/S0040-4039(02)00215-0.
(17) Lazraq, M.; Escudié, J.; Couret, C.; Stagé, J.; Dräger, M.; Dammel, R. *Angew. Chem. Int. Ed. Engl.* **1988**, *27*, 828. doi:10.1002/anie.198808281.
(18) Frisch, M. J.; Trucks, G. W.; Schlegel, H. B.; Scuseria, G. E.; Robb, M. A.; Cheeseman, J. R.; Scalmani, G.; Barone, V.; Mennucci, B.; Petersson, G. A.; Nakatsuji, H.; Caricato, M.; Li, X.; Hratchian, H. P.; Izmaylov, A. F.; Bloino, J.; Zheng, G.; Sonnenberg, J. L.; Hada, M.; Ehara, M.; Toyota, K.; Fukuda, R.; Hasegawa, J.; Ishida, M.; Nakajima, T.; Honda, Y.; Kitao, O.; Nakai, H.; Vreven, T.; Montgomery, J. A., Jr.; Peralta, J. E.; Ogliaro, F.; Bearpark, M.; Heyd, J. J.; Brothers, E.; Kudin, K. N.; Staroverov, V. N.; Kobayashi, R.; Normand, J.; Raghavachari, K.; Rendell, A.; Burant, J. C.; Iyengar, S. S.; Tomasi, J.; Cossi, M.; Rega, N.; Millam, N. J.; Klene, M.; Knox, J. E.; Cross, J. B.; Bakken, V.; Adamo, C.; Jaramillo, J.; Gomperts, R.; Stratmann, R. E.; Yazyev, O.; Austin, A. J.; Cammi, R.; Pomelli, C.; Ochterski, J. W.; Martin, R. L.; Morokuma, K.; Zakrzewski, V. G.; Voth, G. A.; Salvador, P.; Dannenberg, J. J.; Dapprich, S.; Daniels, A. D.; Farkas, Ö.; Foresman, J. B.; Ortiz, J. V.; Cioslowski, J.; Fox, D. J. Gaussian 09, *Revision A1 ed.*; Gaussian Inc.: Wallingford, CT, 2009.